Liquid Crystals

Publication details, including instructions for authors and subscription information:
http://www.informaworld.com/smpp/title~content=t713926090

Liquid crystal molecules with an enyne rigid core

Armand Soldera[a]; Marc-André Beaudoin[a]; Gary O'Brien[a]; Jean Lessard[a]
[a] Chemistry Department, Université de Sherbrooke, Sherbrooke (Québec), Canada

To cite this Article Soldera, Armand , Beaudoin, Marc-André , O'Brien, Gary and Lessard, Jean(2005) 'Liquid crystal molecules with an enyne rigid core', Liquid Crystals, 32: 10, 1223 — 1231

To link to this Article: DOI: 10.1080/02678290500329499

URL: http://dx.doi.org/10.1080/02678290500329499

Liquid Crystals, Vol. 32, No. 10, October 2005, 1223–1231

Taylor & Francis
Taylor & Francis Group

Liquid crystal molecules with an enyne rigid core

ARMAND SOLDERA*, MARC-ANDRÉ BEAUDOIN, GARY O'BRIEN and JEAN LESSARD
Chemistry Department, Université de Sherbrooke, Sherbrooke (Québec), Canada J1K 2R1

(*Received 8 March 2005; accepted 15 July 2005*)

New mesogens are always a source of interest, especially when they possess a non-conventional architecture. In this article are presented the synthesis and polymorphism of a series of compounds possessing a 1,4-diaryl-1-buten-3-yne moiety as the rigid core with an alkoxy chain on each side. Such a core is termed an enyne core. The alkoxy chain is lengthened on each side of the enyne core according to two different fashions: symmetrically and asymmetrically. In this way a rich polymorphism is achieved in some compounds. At lower chain length, the compounds exhibit smectic H and nematic phases where cybotactic groups are observed in X-ray diffraction patterns. As the alkoxy chains extend, smectic C and smectic F phases appear. The non-cylindrical shape of these compounds involves a molecular packing that is preserved throughout the polymorphism. A comparison between symmetric and asymmetric compounds, from X-ray diffraction pattern analysis of their smectic H phases, reveals a parallel molecular stacking. It also discloses the importance of the moiety that is lengthened since different polymorphisms are obtained.

1. Introduction

There are several advantages in obtaining new compounds exhibiting mesophases upon heating. They could provide insight into the intrinsic properties of their liquid crystalline phases. They could display enhanced properties, e.g. higher non-linear optical, NLO, properties [1]. Despite the huge number of liquid crystal compounds identified (more than 90 000 compounds according to LCI publisher), new mesogens are still a source of interest. Nevertheless a specific design procedure has to be pursued. Although hints concerning the polymorphism of new compounds can be inferred from their molecular architecture [2], the complete polymorphism can be gained only by the synthesis of the compounds and their complete characterization. In this article, a new series of mesogenic compounds is reported. Their structure comprises a 1,4-diaryl-1-buten-3-yne rigid core with an alkoxy chain on each side, see figure 1. Throughout the text, the enyne name will designate such a core. The notation used to name these molecules is as follows: *p*DT*n*, where *p* is the number of carbon atoms in the phenyl-double (D) bond moiety, and *n* is the number of carbon atoms in the phenyl-triple (T) bond part. Two kinds of molecules were synthesized: symmetric molecules where the alkoxy chains exhibit the same length on each side of the rigid core (*n*DT*n*, where $n=6$, 8, 10 and 12), and asymmetric molecules where the number of carbon atoms is different on each side of the core (6DT12 and 12DT6). The central bridging enyne group has already been the core of some mesogen molecules but the approaches were different: Soldera synthesized the first reported mesogen molecules with an enyne core [3]; Kitamura *et al.* examined different substituents in one part of the enyne core [4]; Goto *et al.* studied the enyne core with an alkyl chain for its high birefringence [5]; and, Gallardo *et al.* studied piperazine enyne molecules [6]. In this study, the enyne core was primarily designed to exhibit NLO properties.

The enyne core actually derives from the consideration of the properties of the π-conjugated stilbene and tolan groups [7]. These two π-systems are usually inserted in push–pull systems to promote NLO properties. By varying the number of double or triple bonds, i.e. by altering the bond-length alternation, BLA, the value of the first order hyperpolarizability changes [8]. The increase in the BLA inside the π-conjugated system shifts the absorption bands to higher wavelengths (red shift problem) [9]. An alternative to such series of double-single or triple-single bonds, is to obtain compounds with a mixture of single, double, and triple bonds, through a π-conjugated system. Accordingly, the enyne group has been designed. The NLO properties of such compounds will be the subject of subsequent papers. In this paper, the synthesis and liquid crystalline behaviour of four symmetric molecules and two asymmetric molecules is reported.

---

*Corresponding author.
Email: Armand.Soldera@USherbrooke.ca

Liquid Crystals
ISSN 0267-8292 print/ISSN 1366-5855 online © 2005 Taylor & Francis
http://www.tandf.co.uk/journals
DOI: 10.1080/02678290500329499

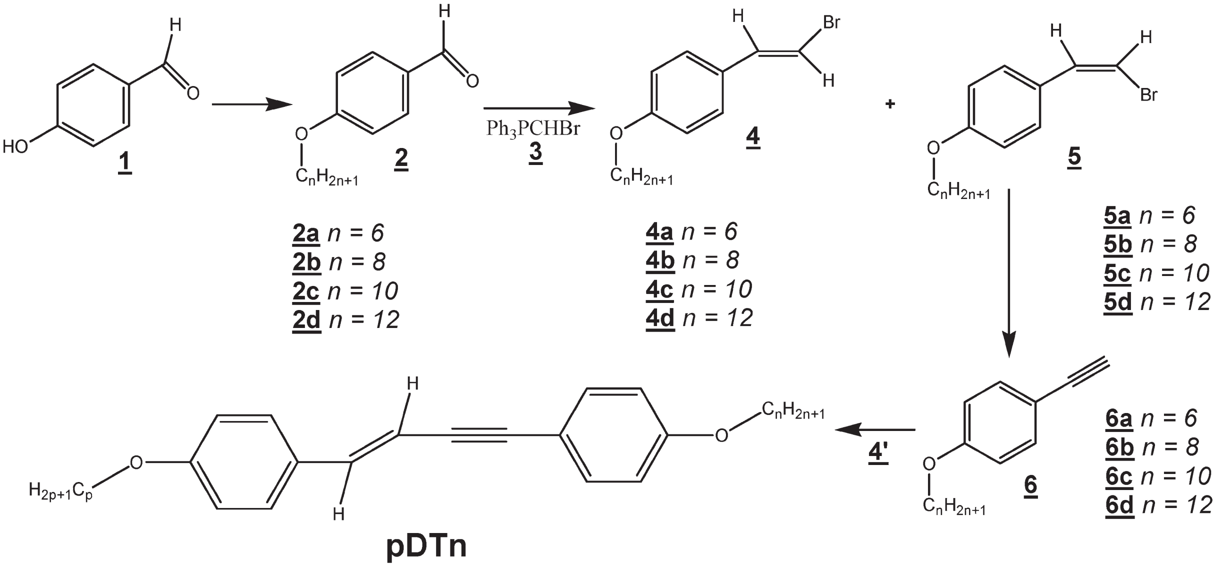

Figure 1. Synthesis scheme for the enyne compounds.

2. Experimental

2.1. *Synthesis*

Dibromomethane and triphenylphosphine were purchased from Alfa Aesar. Sodium hydroxide, 1-bromoalkanes, 4-hydroxybenzaldehyde, potassium *tert*-butoxide, copper(I) iodide, bis(triphenylphosphine)palladium(II) chloride, and triethylamine were purchased from Aldrich Chemicals Co. Toluene was dried over sodium hydride and distilled; THF was dried over sodium metal and distilled. Nuclear magnetic resonance (^{1}H) spectra were obtained with a Bruker AC-300 NMR spectrometer in deuterated chloroform.

The general procedure for synthesis of *p*DT*n* compounds is schematized in figure 1. The synthesis of the enyne molecules is based on the procedure developed by Soldera using a Wittig reaction to obtain the *E* and *Z* forms [3, 10, 11]. Bromide **3** was prepared following the method described by Rodriguez *et al.* [12]. The percentage of each isomer could be varied by changing the nature of the solvent [13]. The two isomers could then be separated to obtain asymmetric enyne compounds, or the mixture used as such to obtain the symmetric enyne compound. The synthesis of the phenylvinyl bromide intermediate, **4**, was reported by Kitamura *et al.*, using three steps from the benzaldehyde [4].

2.1.1. 4-Alkyloxybenzaldehydes, 2.

A typical procedure, the synthesis of 4-hexyloxybenzaldehyde, **2a**, is first presented. In 50 ml of dried ethanol were dissolved 2.2 g (55 mmol) of sodium hydroxide. To this solution were added 6.16 g (50.4 mmol) of 4-hydroxybenzaldehyde, **1**, and 11.4 g (45.8 mmol) of 1-bromohexane. The mixture was heated to reflux and stirred for 4 h. Sodium bromide was filtered off and washed with cold ethanol. The combined ethanol solution was then evaporated under reduced pressure and an aqueous solution of 5% HCl added. The mixture was extracted with ether; the organic phase was dried over anhydrous magnesium sulfate and evaporated in a rotary evaporator. The synthesis of the other 4-alkoxybenzaldehydes was carried out using the same procedure. The purification of 4-hexyloxybenzaldehyde, **2a**, and 4-octyloxybenzaldehyde, **2b**, was carried out by distillation under reduced pressure. 4-Decyloxybenzaldehyde, **2c**, and 4-dodecyloxybenzaldehyde, **4d**, were purified by flash chromatography on silica gel using ethyl acetate in hexane (30/70) as eluent. Transparent to yellowish liquids were obtained in 38–66% yields. ^{1}H NMR ($CDCl_3$): **2a** δ=10.00 (s, 1H), 7.82 (d, 2H, J=8.8 Hz), 6.99 (d, 2H, J=8.4 Hz), 4.03 (t, 2H, J=6.6 Hz), 1.81 (q, 2H, J=6.8 Hz), 1.60–1.10 (m, 6H), 0.91 (t, 3H, J=6.4 Hz); **2b** δ=9.99 (s, 1H), 7.82 (d, 2H, J=8.9 Hz), 7.00 (d, 2H, J=8.6 Hz), 4.0 (t, 2H, J=5.0 Hz), 1.80 (q, 2H, J=7.0 Hz), 1.60–1.10 (m, 10H), 0.91 (t, 3H, J=6.6 Hz); **2c** δ=9.98 (s, 1H), 7.81 (d, 2H, J=8.8 Hz), 7.00 (d, 2H, J=8.5 Hz), 4.0 (t, 2H, J=5.0 Hz), 1.80 (q, 2H, J=6.0 Hz), 1.60–1.10 (m, 14H), 0.91 (t, 3H, J=6.4 Hz); **2d** δ=10.00 (s, 1H), 7.82 (d, 2H, J=8.9 Hz), 7.01 (d, 2H, J=8.7 Hz), 4.0 (t, 2H, J=5.0 Hz), 1.81 (q, 2H, J=7.0 Hz), 1.60–1.10 (m, 18H), 0.91 (t, 3H, J=7.0 Hz).

2.1.2. Bromomethyltriphenylphosphonium bromide, 3. To a stirred solution of 11.9 g (45.2 mmol) of triphenylphosphine in 100 ml of dry toluene under argon was added slowly 15.6 g (89.7 mmol) of dibromomethane. The solution was heated at reflux for 24 h. It was then cooled to −20°C to precipitate bromomethyltriphenylphosphonium bromide, **3**, which was filtered and washed with cold toluene. The filtered solution was heated at reflux for 24 h and an additional amount of **3** was collected by filtration. The two fractions were combined and the solvent evaporated under reduced pressure to afford 10.6 g (55%) of **3** as a pale gray solid, m.p. 230–232°C (lit. 232–235°C [3]). ^{1}H NMR (CDCl$_3$) δ=7.95 (m, 6H), 7.82 (m, 3H), 7.70 (m, 6H), 6.89 (d, 2H, J=6.5 Hz).

2.1.3. 1-(2-Bromovinyl)-4-alkyloxybenzenes, 4 and 5, and 1-ethynyl-4-alkoxybenzenes, 6. A typical procedure, the synthesis of 1-ethynyl-4-hexyloxybenzene, **6a**, is described first. To 200 ml of dry toluene was added 6.11 g (14.0 mmol) of bromomethyltriphenylphosphonium bromide, **3**. The solution was cooled to −78°C, and 1.57 g (14.0 mmol) of potassium *tert*-butoxide was then added under argon; the solution was stirred for 1 h at −78°C. To the yellow solution was added 2.89 g (14.0 mmol) of 4-hexyloxybenzaldehyde, **2a**, and the mixture stirred for 4 h to give the two 1-(2-bromovinyl)-4-hexyloxybenzenes (**4a**, **5a**) with a ratio of *E*/*Z* isomers of 1:2.5, as determined by ^{1}H NMR. An additional 1.57 g (14.0 mmol) of potassium *tert*-butoxide was then added to perform an elimination reaction (the elimination was faster with the *Z* isomer than with the *E* isomer), to give the 1-ethynyl-4-hexyloxybenzene, **6a**. The toluene was removed by evaporation under reduced pressure. An aqueous solution of 5% HCl was added and the mixture was extracted with ether. The organic layer was dried over anhydrous magnesium sulphate. Purification was effected by flash chromatography on silica gel using toluene in hexanes (10/90) as eluent to separate the mixture of olefin isomers from the 1-ethynyl-4-hexyloxybenzene. The other derivatives were synthesized and purified using the same procedure. Transparent oils were obtained in 46–79% total yields. After the elimination reaction, the *E*/*Z* ratio for the various olefins was between 7:3 and 9:1. ^{1}H NMR (CDCl$_3$): **4a** and **5a** (4 : 1 ratio) δ=7.65 (d, **5a**, 2H, J=8.6 Hz), 7.22 (d, **4a**, 2H, J=8.6 Hz), 7.03 (d, **4a**, 1H, J=14.0 Hz), 6.98 (d, **5a**, 1H, J=8.8 Hz), 6.90 (d, **5a**, 2H, J=8.6 Hz), 6.83 (d, **4a**, 2H, J=8.6 Hz), 6.60 (d, **4a**, 1H, J=14.0 Hz), 6.29 (d, **5a**, 1H, J=8.8 Hz), 3.95 and 3.90 (2 t, **4a** and **5a**, 4H, J=6.6 Hz), 1.90–1.20 (m, **4a** and **5a**, 16H), 0.91 (t, **4a** and **5a**, 6H, J=7.2 Hz); **4b** and **5b** (6 : 1 ratio) δ=7.65 (d, **5b**, 2H, J=8.6 Hz), 7.22 (d, **4b**, 2H, J=8.6 Hz), 7.03 (d, **4b**, 1H, J=13.9 Hz), 6.99 (d, **5b**, 1H, J=8.5 Hz), 6.90 (d, **5b**, 2H, J=8.6 Hz), 6.83 (d, **4b**, 2H, J=8.6 Hz), 6.59 (d, **4b**, 1H, J=13.9 Hz), 6.30 (d, **5b**, 1H, J=8.5 Hz), 3.96 and 3.90 (2 t, **4b** and **5b**, 4H, J=6.3 Hz), 1.90–1.20 (m, **4b** and **5b**, 24H), 0.91 (t, **4b** and **5b**, 6H, J=7.1 Hz); **4c** and **5c** (7 : 3 ratio) δ=7.65 (d, **5c**, 2H, J=8.6 Hz), 7.22 (d, **4c**, 2H, J=8.6 Hz), 7.03 (d, **4c**, 1H, J=14.7 Hz), 6.99 (d, **5c**, 1H, J=8.7 Hz), 6.90 (d, **5c**, 2H, J=8.6 Hz), 6.83 (d, **4c**, 2H, J=8.6 Hz), 6.60 (d, **4c**, 1H, J=14.7 Hz), 6.30 (d, **5c**, 1H, J=8.7 Hz), 3.96 and 3.90 (2 t, **4c** and **5c**, 4H, J=6.3 Hz), 1.90–1.20 (m, **4c** and **5c**, 32H), 0.91 (t, **4c** and **5c**, 6H, J=7.1 Hz); **4d** and **5d** (9 : 1 ratio) δ=7.65 (d, **5d**, 2H, J=8.6 Hz), 7.22 (d, **4d**, 2H, J=8.6 Hz), 7.03 (d, **4d**, 1H, J=14.3 Hz), 6.99 (d, **5d**, 1H, J=9.1 Hz), 6.90 (d, **5d**, 2H, J=8.6 Hz), 6.83 (d, **4d**, 2H, J=8.6 Hz), 6.59 (d, **4d**, 1H, J=14.3 Hz), 6.29 (d, **5d**, 1H, J=9.1 Hz), 3.96 and 3.90 (2 t, **4d** and **5d**, 4H, J=6.2 Hz), 1.90–1.20 (m, **4d** and **5d**, 40H), 0.91 (t, **4d** and **5d**, 6H, J=7.0 Hz); **6a** δ=7.45 (d, 2H, J=8.4 Hz), 6.84 (d, 2H, J=8.4 Hz), 3.96 (t, 2H, J=6.2 Hz), 2.98 (s, 1H), 1.80 (q, 2H, J=6.9 Hz), 1.70–1.20 (m, 6H), 0.9 (t, 3H, J=7.3 Hz); **6b** δ=7.45 (d, 2H, J=8.6 Hz), 6.84 (d, 2H, J=7.2 Hz), 3.95 (t, 2H, J=6.7 Hz), 2.99 (s, 1H), 1.78 (q, 2H, J=6.7 Hz), 1.70–1.20 (m, 10H), 0.9 (t, 3H, J=7.1 Hz); **6c** δ=7.42 (d, 2H, J=8.7 Hz), 6.84 (d, 2H, J=8.7 Hz), 3.96 (t, 2H, J=6.2 Hz), 2.99 (s, 1H), 1.81 (q, 2H, J=6.5 Hz), 1.70–1.20 (m, 14H), 0.90 (t, 3H, J=7.9 Hz); **6d** δ=7.43 (d, 2H, J=8.7 Hz), 6.84 (d, 2H, J=8.7 Hz), 3.96 (t, 2H, J=6.2 Hz), 2.99 (s, 1H), 1.82 (q, 2H, J=6.7 Hz), 1.70–1.20 (m, 18H), 0.92 (t, 3H, J=6.9 Hz).

2.1.4. Symmetric 1,4-di(4-alkyloxyphenyl)-but-1-en-3-ynes, *n*DT*n*. The mixture of *Z* and *E* isomers of 1-(2-bromovinyl)-4-octyloxybenzene, **4b** and **5b** (0.40 g, 1.4 mmol), and 1-ethynyl-4-octyloxybenzene, **6b** (0.34 g, 1.5 mmol), was dissolved in 3 ml of dry THF and 1.45 ml (10.7 mmol) of triethylamine under an atmosphere of argon. Copper(I) iodide (29 mg) and dichlorobis(triphenylphosphine)palladium(II) (44 mg) were added to the solution. The black mixture was stirred at 40–50°C for 24 h. After cooling, the precipitate was filtered off, washed with cold THF and the solvent eliminated by evaporation. The crude product was purified by column chromatography on silica gel using toluene in hexanes (25/75) as eluent, followed by recrystallization from isopropanol/hexanes. White crystals were obtained in 12–52% yields. ^{1}H NMR (CDCl$_3$): **6DT6** δ=7.38 (d, 2H, J=8.5 Hz), 7.34 (d, 2H, J=8.8 Hz), 6.93 (d, 1H, J=16.0 Hz), 6.84 (d, 2H, J=9.9 Hz), 6.82 (d, 2H, J=9.4 Hz), 6.21 (d, 1H, J=16.0 Hz), 3.97 (t, 4H, J=6.6 Hz), 1.79 (q, 4H,

$J=7.0$ Hz), 1.60–1.10 (m, 12H), 0.91 (t, 6H, $J=7.0$ Hz); **8DT8** $\delta=7.38$ (d, 2H, $J=9.4$ Hz), 7.33 (d, 2H, $J=9.9$ Hz), 6.96 (d, 1H, $J=15.8$ Hz), 6.84 (d, 2H, $J=9.9$ Hz), 6.82 (d, 2H, $J=9.4$ Hz), 6.22 (d, 1H, $J=15.8$ Hz), 3.96 (t, 4H, $J=6.6$ Hz), 1.78 (q, 4H, $J=7.2$ Hz), 1.60–1.10 (m, 20H), 0.92 (t, 6H, $J=7.1$ Hz); **10DT10** $\delta=7.39$ (d, 2H, $J=9.5$ Hz), 7.34 (d, 2H, $J=10.0$ Hz), 6.95 (d, 1H, $J=16.3$ Hz), 6.86 (d, 2H, $J=10.0$ Hz), 6.84 (d, 2H, $J=9.5$ Hz), 6.23 (d, 1H, $J=16.3$ Hz), 3.96 (t, 4H, $J=6.8$ Hz), 1.78 (q, 4H, $J=7.2$ Hz), 1.60–1.10 (m, 28H), 0.91 (t, 6H, $J=7.0$ Hz); **12DT12** $\delta=7.38$ (d, 2H, $J=8.6$ Hz), 7.34 (d, 2H, $J=9.7$ Hz), 6.94 (d, 1H, $J=16.0$ Hz), 6.86 (d, 2H, $J=9.7$ Hz), 6.83 (d, 2H, $J=8.6$ Hz), 6.25 (d, 1H, $J=16.0$ Hz), 3.96 (t, 4H, $J=6.7$ Hz), 1.77 (q, 4H, $J=7.1$ Hz), 1.60–1.10 (m, 36H), 0.91 (t, 6H, $J=6.9$ Hz).

2.1.5. Asymmetric 1,4-di(4-alkyloxyphenyl)-but-1-en-3-ynes, *p*DT*n*.

Asymmetric 1,4-di(4-alkyloxyphenyl)-but-1-en-3-ynes were prepared following the procedure used for symmetric enyne molecules. ^{1}H NMR ($CDCl_3$): **6DT12** $\delta=7.38$ (d, 2H, $J=8.1$ Hz), 7.34 (d, 2H, $J=8.7$ Hz), 6.94 (d, 1H, $J=15.7$ Hz), 6.86 (d, 2H, $J=8.7$ Hz), 6.83 (d, 2H, $J=8.1$ Hz), 6.25 (d, 1H, $J=15.7$ Hz), 3.96 (t, 4H, $J=6.8$ Hz), 1.78 (q, 4H, $J=7.1$ Hz), 1.60–1.10 (m, 24H), 0.92 (t, 6H, $J=7.0$ Hz); **12DT6** $\delta=7.38$ (d, 2H, $J=8.9$ Hz), 7.34 (d, 2H, $J=8.7$ Hz), 6.94 (d, 1H, $J=16.2$ Hz), 6.86 (d, 2H, $J=8.7$ Hz), 6.83 (d, 2H, $J=8.9$ Hz), 6.25 (d, 1H, $J=16.2$ Hz), 3.96 (t, 4H, $J=6.7$ Hz), 1.79 (q, 4H, $J=7.0$ Hz), 1.60–1.10 (m, 24H), 0.91 (t, 6H, $J=7.0$ Hz).

2.2. *Characterization*

Investigation of the phase transition temperatures was carried out using differential scanning calorimetry (DSC), polarizing optical microscopy (POM), and X-ray diffraction (XRD). The DSC measurements were performed using a DSC 7 Perkin–Elmer apparatus. Textural observations were made under a polarizing microscope (Leica) connected to a hot stage (FP 82). XRD patterns were obtained from a Siemens/Bruker instrument with a Kristalloflex 760 generator (Cu-$K_{\alpha1}=1.542$ Å).

3. Mesomorphic properties

Results concerning the polymorphism of the six enyne compounds are illustrated in figure 2, and table 1. The results are discussed according to the symmetry of the molecules: § 3.1 concerns the symmetric compounds (6DT6, 8DT8, 10DT10, 12DT12), while the asymmetric compounds (12DT6, 6DT12) are discussed in § 3.2.

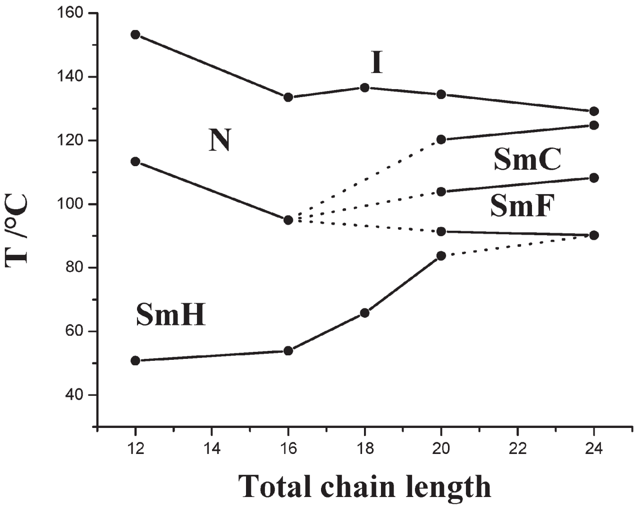

Figure 2. Plot of transition temperature with respect to total chain length of the enyne molecules.

3.1. *Symmetric molecules*

3.1.1. DSC studies. The DSC curves reveal first order transitions and, accordingly, the number of mesophases. Onset temperatures and transition enthalpies are reported in table 1. These data were obtained during the second heating and second cooling at a rate of 10°C min^{-1}. Compounds 6DT6 and 8DT8 exhibit two mesophases, 10DT10 displays four, and 12DT12 three mesophases. All these mesophases are enantiotropic. The transition enthalpy at the clearing point ranges from 4.3 to 5 J g^{-1}, a value that is usually observed for a nematic–liquid transition [14]. The presence of the nematic phase is corroborated by the decrease in its thermal stability as the alkoxy chains are lengthened [15]. Concerning the other transitions, only in the case of 6DT6 is the value of the crystal–mesophase transition enthalpy lower than those of the ensuing transition enthalpies. The reason for this difference may stem from the small chain lengths in the 6DT6 molecule, which would result in stronger intermolecular attractions between the cores. These non-bonded interactions are preserved to a large extent in an orderly mesophase. Consequently, the lower mesophase observed in the case of 6DT6 has to be an orderly mesophase.

3.1.2. Texture investigation. Texture investigation clearly confirms the presence of the nematic phase at higher temperatures [16]. For example, in figure 3 (*a*) 6DT6 at 135°C shows a schlieren texture, revealing the presence of the nematic phase. On decreasing the temperature, an orderly smectic phase is obtained for 6DT6 and 8DT8, but this phase could not be clearly identified. For 10DT10 and 12DT12, paramorphotic

Table 1. Transition temperatures in °C and enthalpies in J g^{-1} (in italics) for the *n*DT*n* series (*n*=6, 8, 10, 12), and for compounds 6DT12 and 12DT6. The heating and cooling rates were 10°C min^{-1}. Cr=crystalline phase; I=isotropic phase. Brackets indicate temperatures and transition enthalpies obtained on cooling.

Compound	Cr		SmH		SmF		SmC		N		I
6DT6	•	50.7	•	113.4	—		—		•	153.2	•
		29		*48*						*4.2*	
	•	(40.7)	•	(110.9)	—		—		•	(151.7)	•
		(−23)		*(−48)*						*(−4.5)*	
8DT8	•	53.8	•	95.0	—		—		•	133.6	•
		60		*33*						*2.6*	
	•	(48.5)	•	(97.2)	—		—		•	(134.2)	•
		(−59)		*(−33)*						*(−2.9)*	
6DT12	•	69.8	•	86.7	•	93.2	•	105.4	•	135.8	•
		56		*11*		*7.8*		*2.4*		*4.3*	
	•	(44.8)	•	(84.7)	•	(99.8)	•	(103.5)	•	(133.9)	•
		(−49)		*(−11)*		*(−10)*		*(−3)*		*(−4.4)*	
12DT6	•	65.8	—	65.8	•	102.3	•	113.1	•	136.6	•
		78		*78*		*10.7*		*3.3*		*5*	
	•	(44.2)	•	(66.7)	•	(99.8)	•	(110.9)	•	(133.9)	•
		(−49)		*(−7)*		*(−10)*		*(−3)*		*(−4.4)*	
10DT10	•	83.8	•	91.4	•	103.9	•	120.3	•	134.4	•
		84		*9.5*		*8.3*		*4.4*		*4.5*	
	•	(78.2)	•	(88.4)	•	(101.3)	•	(117.8)	•	(132.2)	•
		(−88)		*(−11)*		*(−7.7)*		*(−4.3)*		*(−5)*	
12DT12	•	90.2	—		•	108.2	•	124.8	•	129.1	•
		116				*11.3*		*6.2*		*4.9*	
	•	(85.9)	—		•	(105.9)	•	(122.4)	•	(126.8)	•
		(−120)				*(−10.8)*		*(−5.1)*		*(−6.1)*	

schlieren textures are obtained, indicating the formation of a smectic C phase; in figure 3 (*b*), the texture of 10DT10 at 115°C is shown. At 102°C, the texture of 10DT10, figure 3 (*c*), is also of paramorphotic nature: a schlieren-mosaic type texture is exhibited, which derives from the schlieren texture of the smectic C phase. Such a texture can be attributed to a smectic F or smectic I mesophase. An orderly mesophase, at lower temperatures, cannot be unequivocally recognized; X-ray diffraction analysis is thus necessary to identify these mesophases.

3.1.3. X-ray diffraction studies. In this work, no orientation of the molecules using a magnetic field has been carried out. However, XRD patterns in the nematic phase clearly indicate an order that is actually due to the presence of cybotactic groups. As an example, the diffraction pattern of 8DT8 at 120°C is displayed in figure 4. As mentioned by de Vries [17], no sharp peak could be observed in the absence of a magnetic field. The presence of these cybotactic groups can be considered as a pre-transitional phenomenon, indicating that the smectic C phase is easily formed. Such a propensity for a tilted mesophase can be correlated to the crystal structure of these compounds. The crystal structures of 8DT8, 10DT10, and 12DT12 belong to the same crystal system, the monoclinic *Pa* phase; crystal structure parameters are presented in table 2. No further information on crystal packing has been obtained because of the difficulty in obtaining small crystallites.

Compound 10DT10 provides a good example of the range of mesophases to be found in these enyne compounds (it exhibits the maximum number, four). On decreasing the temperature from the nematic phase, XRD patterns clearly show a disordered smectic phase that confirms the texture analysis. The smectic C (and smectic A) phase is characterized by a sharp peak at low *q* and a diffuse peak at higher *q* [15]. To calculate the tilt angle, the molecular length was deduced from the length of the elongated molecular structure calculated by molecular modelling to which was added 2 Å. This additional length corresponds to twice the hydrogen atom radius. The values of the tilt angle can then be determined. The tilt angle variation of 10DT10 in the smectic C phase with respect to temperature is shown in figure 5. It can be seen that the tilt angle, and therefore the interlamellar distance, shows no significant variation with temperature. The tilt angle ranges between 43.6° and 44.7°; these values are in agreement with reported values for the tilt angle in the smectic C phase when a nematic phase is found at a slightly higher temperature [18, 19]. The smectic C phase is also observed in the 12DT12 polymorphism, with a tilt angle

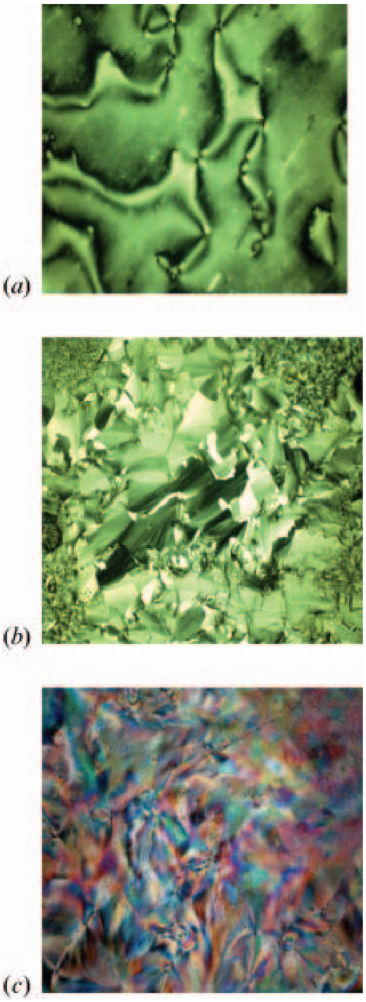

Figure 3. Photomicrograph of the texture of (*a*) 6DT6 at 135°C, (*b*) 10DT10 at 115°C, (*c*) 10DT10 at 102°C.

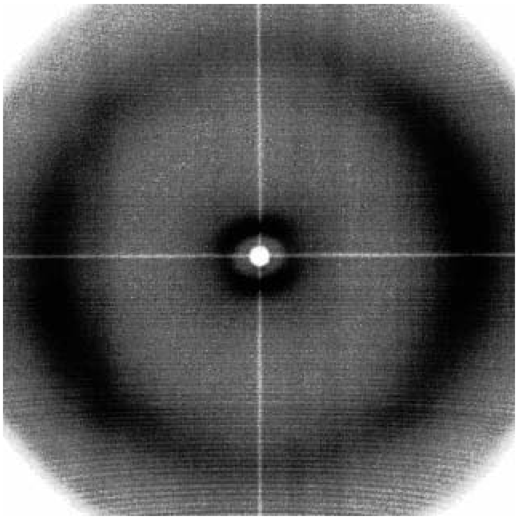

Figure 4. X-ray diffraction pattern of 8DT8 at 120°C, revealing the presence of cybotactic groups.

Table 2. Cell parameters of the crystalline structures of 8DT8, 12DT6, 10DT10 and 12DT12.

Compound	Space group	*a*/Å	*b*/Å	*c*/Å	*β*/°
8DT8	*Pa*	6.193	7.381	31.783	94.87
12DT6	*Pa*	6.2538	7.4331	33.583	93.59
10DT10	*Pa*	6.1076	7.3845	36.391	91.64
12DT12	*Pa*	7.3895	6.017	46.185	93.52

of 44.8°, as deduced from XRD. The appearance of this mesophase in the polymorphism of the 10DT10 and 12DT12 is in agreement with the presence of cybotactic groups in the nematic phase of compounds with a shorter chain length (6DT6 and 8DT8).

For compound 10DT10 at a temperature below the smectic C phase, i.e. below the transition located at 101.3°C, the tilt angle decreases to a value which varies from 34.7° to 33.7°, according to the temperature. This value departs markedly from the tilt angle value in the smectic C phase, as shown in figure 5. The high q region also reveals a second difference between the two tilted mesophases. The diffusion peak is less diffuse than in the case of the smectic C phase. No sharp peak is actually observed, showing that no long distance correlation exists [20]. Nevertheless the difference in peak width discloses a correlation between molecules in the smectic planes, a correlation which does not exist in the smectic C phase [21]. This observation is in agreement with the presence of a hexactic mesophase, as deduced from the texture analysis. To identify the hexactic mesophase, the correlation length, ξ, associated with the diffusion peak at high q was measured. This peak was fitted by a Lorentzian function in the

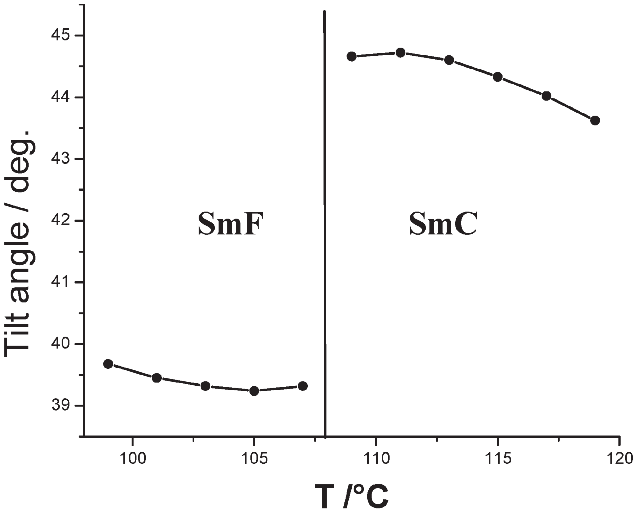

Figure 5. Plot of the tilt angle in the smectic F and smectic C phases of 10DT10, with respect to temperature.

reciprocal space. The FWHM (full width at half maximum), ω, directly leads to ξ through the relationship $\xi=4/\omega$ [22].

The average values of the correlation length for 10DT10 and 12DT12 are reported in table 3; at 3°C below the transition to the SmC phase, ξ is almost constant. The average values of ξ thus obtained are 57.5 ± 0.5 Å, and 63.7 ± 0.5 Å for 10DT10 and 12DT12, respectively. Comparing these values with those found in the literature where the Lorentzian method has also been applied [23], this mesophase is identified as a smectic F phase [21, 24]. The smectic I phase exhibits higher correlation length. The molecular positions in the smectic F phase are uncorrelated. Nevertheless, the molecules are tilted in an edge of the pseudo-hexagonal molecular packing ($a>b$).

While for 12DT12, the lower temperature mesophase is the smectic F phase, the other three compounds exhibit the same diffraction pattern for the low temperature mesophase. A series of sharp peaks appears in the high q region indicating an orderly smectic phase. Since the crystal system of the solid phase is monoclinic, and all the higher temperature mesophases are tilted, the diffraction peaks are assumed to correspond to an orderly tilted smectic phase. Due to the small number of peaks (a maximum of five peaks in the high q region is found for 8DT8), a specific procedure based on published results on orderly tilted smectic phases was undertaken. Since highly ordered crystalline smectic phases keep the memory of the order present in the solid phase, it is inferred that the low temperature mesophase is of *Pa* symmetry [25]. The XRD pattern of this mesophase may be compared with those of the orderly smectic phases of TBBA reported by Doucet *et al.* [26]. Phase VI, i.e. smectic H (*Pa* symmetry), exhibits a comparable pattern: two major peaks are observed (figure 6). The most intense peak is attributed to the (1 1 0) reflection, while the other is ascribed to the (2 0 0) reflection [26]. The b cell parameter may thus be deduced. Considering the computed molecular length, the position of the (0 0 1) reflection located in the low q region, automatically yields the β angle value. The value of the a parameter may thus be inferred from the position of the (2 0 0) reflection. The other reticular planes are thus obtained. The powder XRD pattern of 8DT8 obtained at 90°C, is shown in figure 6. The Miller indices of the corresponding reticular planes of diffraction are also shown in this figure. Their presence is in agreement with the extinction rule of the smectic H phase [20]. The attribution of cell parameters is shown in table 3.

3.2. *Asymmetric molecules*

The polymorphisms of 6DT12 and 12DT6 were deduced from the previous analysis on the symmetric compounds. Compound 12DT6 exhibits three enantiotropic mesophases, and one additional monotropic mesophase, while 6DT12 shows four enantiotropic mesophases. The two compounds exhibit comparable transition temperatures from the crystalline structure

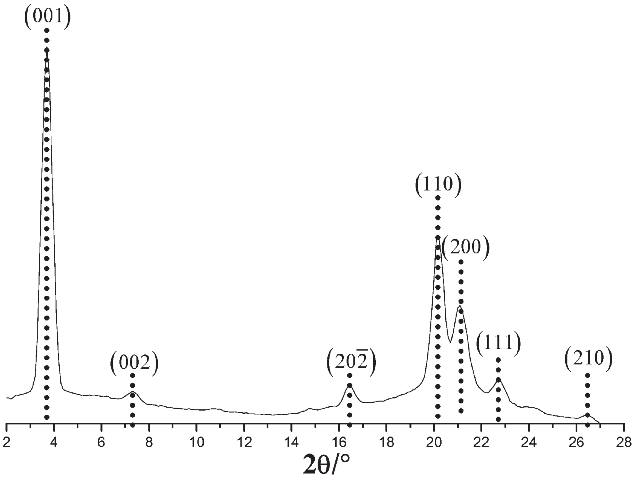

Figure 6. X-ray diffraction plot of the smectic H phase of 8DT8 at 90°C; the Miller indices of the reflection planes are shown.

Table 3. Correlation length in the smectic F phase, and smectic H cell parameters for the nDTn series (n=6, 8, 10, 12), and for compounds 6DT12 and 12DT6.

	SmF	SmH				
Compound	ξ (T)/Å	a/Å	b/Å	c/Å	β/°	Molecular length/ Å
6DT6	—	13.8	5.16	33.1	142.9	33.1
8DT8	—	13.5	5.15	38.1	141.4	38.1
6DT12	42.8 Å	13.1	5.18	41.0	140.1	41.0
12DT6	79.9 ± 0.5 Å	—	—	—	—	41.0
10DT10	57.5 ± 0.3 Å	13.2	5.0	43.3	142.6	43.3
12DT12	63.7 ± 0.5 Å	—	—	—	—	48.3

and to the isotropic liquid (table 1). However, the temperatures of transition between mesophases are different; for the sake of clarity they are not shown in figure 2. From XRD analysis, the low temperature mesophase of 12DT6 was found to be a smectic F phase; the correlation length is shown in table 3. The monotropic mesophase could not be isolated, but having regard to results stemming from analysis of the symmetric compounds, it is assumed that it is a smectic H phase. This compound thus presents a Cr–(SmH)–SmF–SmC–N–I polymorphism. The polymorphism of 6DT12 is Cr–SmH–SmF–SmC–N–I, see table 3. The procedure to establish that the compound exhibits the smectic H phase in 6DT12 was described in § 3.1.3. Concerning the smectic C phase, the tilt angle value is also in agreement with published results: 42° for both asymmetric compounds. The correlation length for 12DT6 is the greatest of all these compounds, 76 Å, as shown in table 3. The ξ value is, in fact, greatly affected by the sample preparation [23].

4. Discussion

Four of the newly described compounds exhibit the monotropic smectic H phase: 6DT6, 8DT8, 6DT12 and 10DT10. The detailed crystallographic data are shown in table 3. The a and c parameters, as well as the angle β, depend on molecular length; the c parameter usually corresponds to the molecular length [20]. The b parameter is almost constant for the four compounds, although slightly different for 10DT10; this small difference can be due to the difficulty in isolating the smectic H phase, with resulting poor resolution. The projection of the a edge perpendicular to the molecular axis, a_p, does not vary on increasing the number of carbon atoms in the molecules (8.4 Å). Accordingly, the lateral intermolecular interactions are of the same order of magnitude for all the compounds; the molecular packing is therefore the same. The projections of the a edge along the molecular axis, a_c, changes slightly from 11 to 10 Å between compounds 6DT6 and 6DT12. Consequently, as proposed by de Vries and Fishel [27], there is a difference of $a_c/2$, i.e. 5.5 to 5 Å, between two molecules along the a direction. If the molecules are arranged in anti-parallel packing, there would be a net variation in the cell parameters. For example, 6DT12 would exhibit cell parameters depicting higher chain length behaviour, but it exhibits smectic H cell parameters comparable to the symmetric compound. Consequently, the arrangement of parallel stacking molecules is favoured.

Considering that interactions between dipole moments are weak, the major interactions stem from phenylene groups. These weak interactions are also deduced from the fact that the nematic phase is still preserved in the polymorphism of 12DT12, which possesses a total chain length of 24 carbon atoms. This indicates that the lateral intermolecular attractions are weak, but terminal non-bonded interactions predominate [16]. As suggested by de Vries [28], those ‘phenylene interactions’ tend to arrange the phenylene groups in herringbone-type packing. Such interactions actually yield to the Pa symmetry in the crystal structure of these molecules. A detailed study of interactions between the cores is at present being carried out using molecular modelling simulations.

The smectic H analysis yielded information on the parallel packing of the molecules. Such information is essential for subsequent studies on the polymorphism of the enyne compounds. The crystal–smectic and nematic–isotropic transition temperatures of all the compounds (symmetric and asymmetric) with respect to the number of carbon atoms in the alkoxy chains are reported in figure 2; smooth curves are obtained. As the chains lengthen, both the distance between the polarizable cores and the overall polarizability increase. This is why the 6DT12 and 12DT6 crystal–mesophase transition temperatures and the clearing points fall on the same smooth curve, since the total chain length (18 atoms of carbon) between two consecutive cores is the same and is even, as in the case of symmetric molecules. Nevertheless as mentioned by Gray *et al.* [16], the mesomorphic transitions are more closely related to the chemical difference. Thus, 6DT12 and 12DT6 exhibit different polymorphisms with different mesophase transition temperatures: four enantiotropic mesophases for 6DT12, and three enantiotropic mesophases for 12DT6 (and one monotropic). So, for the sake of clarity, these transitions are not shown in figure 2. The difference in polymorphism between the two asymmetric compounds is thus of particular interest, since it gives information on the contribution of each enyne core moiety.

The polymorphism of the two asymmetric compounds can in fact be linked with that of the symmetric compounds: 12DT6 and 12DT12 form a pair of compounds that do not exhibit the smectic H phase in their polymorphism; the other pair, 6DT12 and 6DT6, comprises smectogen H molecules. From a molecular viewpoint, the two pairs are differentiated by the length of the alkoxy chain in the double bond moiety: the former pair is characterized by a long alkoxy chain in the double bond moiety, while the latter pair exhibits a short alkoxy chain. It is only in the pair with the short alkoxy chain associated with the double bond that the smectic H phase appears. Consequently, lateral intermolecular attractions are stronger between the double bond moieties than between the triple bond moieties. This difference could be explained by the larger polarizability of the stilbene molecule in comparison with the tolane moiety. Nevertheless as the temperature is decreased, the thermal stability of the smectic F phase is lower for 6DT12. This lower thermal stability is confirmed by the appearance of the nematic phase at a temperature 7°C lower for 6DT12 than for the 12DT6. At these temperatures, the flexibility of the chain attached to the tolane segment has a greater impact on the thermal stability of the mesophases. A parallel with the simple stilbene and tolane molecules cannot simply be drawn. Several questions must be addressed before any conclusion on the nature of such interactions can be made. Does the pedal motion in stilbene molecules still exist in the enyne compound [29, 30]? How do the molecules pack together? To answer those questions, molecular simulations are at present being carried out.

5. Conclusions

The presence of the enyne core imparts interesting polymorphisms to the new series of compounds. At higher temperatures, cybotactic groups are observed. These groups are actually pretransitional effects, indicating that the smectic C phase will appear. This phase is actually observed for a compound with a total alkoxy chain length of 18 carbon atoms. Additional tilted mesophases are also obtained: the smectic F and smectic H phases. The packing of the molecules is thus preserved throughout the polymorphism. Such a molecular stacking is due to the particular non-cylindrical shape of the enyne structure. Moreover, the polymorphism is greatly affected by the moieties 1,4-aryl-butene or 1,4-aryl-butyne, in which the chain length is increased. This work pave the way for further studies.

Acknowledgment

Financial support for this work from NSERC and Université de Sherbrooke (through the program of Groupe d'Excellence: Centre d'Études des Matériaux en Optique et Photonique de l'Université de Sherbrooke, CÉMOPUS) is gratefully acknowledged. We would also like to thank Prof. Yue Zhao, of Université de Sherbrooke, for access to his laboratory, Dr. Daniel Fortin for the structure determination of the crystalline phases, and CERSIM and Dr. Rodica Plesu for the X-ray diffraction patterns of the mesophases.

References

[1] A. Soldera, R. Theberge. *Liq. Cryst.*, **30**, 1251 (2003).
[2] D. Demus. *Mol. Cryst. liq. Cryst.*, **165**, 45 (1988).
[3] A. Soldera. PhD thesis, Université Louis Pasteur, Strasbourg (1992).
[4] Y. Kitamura, Y. Aoyagi, Y. Fujiwara. *Chem. Lett.*, 1271 (1998).
[5] Y. Goto, T. Inukai, A. Fujita, D. Demus. *Mol. Cryst. liq. Cryst.*, **260**, 23 (1995).
[6] H. Gallardo, L. Maurmann. *Mol. Cryst. liq. Cryst.*, **378**, 23 (2002).
[7] W. Bartkowiak, R. Zaleny, W. Niewodniczaski, J. Leszczynski. *J. phys. Chem. A.*, **105**, 10702 (2001).
[8] B.J. Coe. *Chem. Eur. J.*, **5**, 2464 (1999).
[9] M.S. Wong, Z.H. Li, Y. Tao, M. D'iorio. *Chem. Mater.*, **15**, 1198 (2003).
[10] M. Matsumoto, K. Kuroda. *Tetrahedron Lett.*, **21**, 4021 (1980).
[11] J. Wolinsky, K.L. Erickson. *J. org. Chem.*, **30**, 2208 (1965).
[12] J.G. Rodriguez, R. Martin-Villamil, A. Lafuente. *Tetrahedron*, **59**, 1021 (2003).
[13] B.P. Andreini, M. Benetti, A. Carpita, R. Rossi. *Gazz. Chem. Ital.*, **118**, 469 (1988).
[14] T. Bellini, N.A. Clark, C.D. Muzny, L. Lu, C.W. Garland, D.W. Schaefer, B.J. Oliver. *Phys. Rev. Lett.*, **69**, 788 (1992).
[15] G.W. Gray. *Molecular Structure and the Properties of Liquid Crystals*, Academic Press, London (1962).
[16] G.W. Gray, J.W. Goodby. *Smectic Liquid Crystals: Textures and Structures*, Leonard Hill, Glasgow (1984).
[17] A. de Vries. *J. mol. Liq.*, **31**, 193 (1986).
[18] A.M. Biradar, S.S. Bawa, S. Chandra. *Phys. Rev. A*, **45**, 7282 (1992).
[19] W.L. Mcmillan. *Phys. Rev. A*, **8**, 328 (1973).
[20] A. de Vries. *J. chem. Phys.*, **70**, 2705 (1979).
[21] J.J. Benattar, F. Moussa, M. Ambert. *J. Physique. Lett.*, **42**, L67 (1981).
[22] A.J. Leadbetter. *The Molecular Physics of Liquid Crystals*, Academic Press, London (1979).
[23] P.A.C. Gane, A.J. Leadbetter, P.G. Wrighton. *Mol. Cryst, liq. Cryst.*, **66**, 247 (1981).
[24] L.M. Blinov, T.A. Lobko, B.I. Ostrovskii, S.N. Sulianov, F.G. Tournilhac. *J. Phys. II Fr.*, **3**, 1121 (1993).
[25] W. Haase, M.A. Athanassopoulou. *Struct. Bonding*, **94**, 139 (1999).
[26] J. Doucet, A.M. Levelut, M. Lambert. *Phys. Rev. Lett.*, **32**, 301 (1974).
[27] A. de Vries, D.L. . Fishel. *Mol. Cryst. liq. Cryst.*, **16**, 311 (1972).
[28] A. de Vries. *J. chem. Phys.*, **61**, 2367 (1974).
[29] J. Harada, K. Ogawa. *J. Am. Chem. Soc.*, **123**, 10884 (2001).
[30] S. Galli, P. Mercandelli, A. Sironi. *J. Am. chem. Soc.*, **121**, 3767 (1999).